A Protection Strategy for Micro-Grids Based on Positive-Sequence Impedance

Sohrab Mirsaeidi, Dalila Mat Said, Mohd. Wazir Mustafa,
Mohd. Hafiz Habibuddin and Kimia Ghaffari

ABSTRACT

In recent years, the concept of micro-grid has appeared as an appropriate way for the integration of Distributed Energy Resources (DERs) in the distribution networks. However, micro-grids have encountered a number of challenges from control and protection aspects. One of the main issues relevant to the protection of micro-grids is to develop a suitable protection technique which is effective in both grid-connected and stand-alone operation modes. This article presents a new micro-grid protection strategy based on positive-sequence impedance using Phasor Measurement Units (PMUs) and a designed Microprocessor-Based Relay (MBR) along with a narrowband communication system (only to exchange digital information, not electrical power). The main attribution of the proposed scheme is that it has the ability to protect micro-grids containing either radial or looped feeders; additionally, the capabilities of automatic updating of pick-up threshold value and single-phase tripping have been considered in the designed MBR. Finally, in order to verify the effectiveness of the suggested scheme and the designed MBR, several simulations have been undertaken by using DIgSILENT PowerFactory and Matlab software packages.

Keywords: Micro-grid protection, grid-connected mode, islanded mode, positive-sequence component.

INTRODUCTION

Advances in technology and the increasing concerns associated with global warming have motivated researchers to explore cleaner and more efficient systems. In order to mitigate the negative influences of fossil fuel based generation upon the environment, a novel approach is to produce electricity by cleaner Distributed Energy Resources (DERs) in the vicinity of the customers' sites [1-3]. For this reason, the utilization of DERs such as wind turbines, photovoltaic systems, micro gas turbines and fuel cells has attracted more attention in recent years.

One suggested way for the integration of widespread proliferation of DERs is through micro-grids. Micro-grid is substantially defined as a collection of electrical/heat loads, parallel DERs and energy storage devices which can function in synchronism with the main grid (grid-connected mode) or in isolation from the remainder of the distribution network (islanded mode) [4-7]. The micro-grid protection philosophy is that it functions in grid-connected mode of operation under normal circumstances, but in case a fault takes place in the main grid side, it is disconnected from the rest of the network at the Point of Common Coupling (PCC) and is transferred to the islanded mode [8-10]. Figure 1 shows the structure of a typical micro-grid.

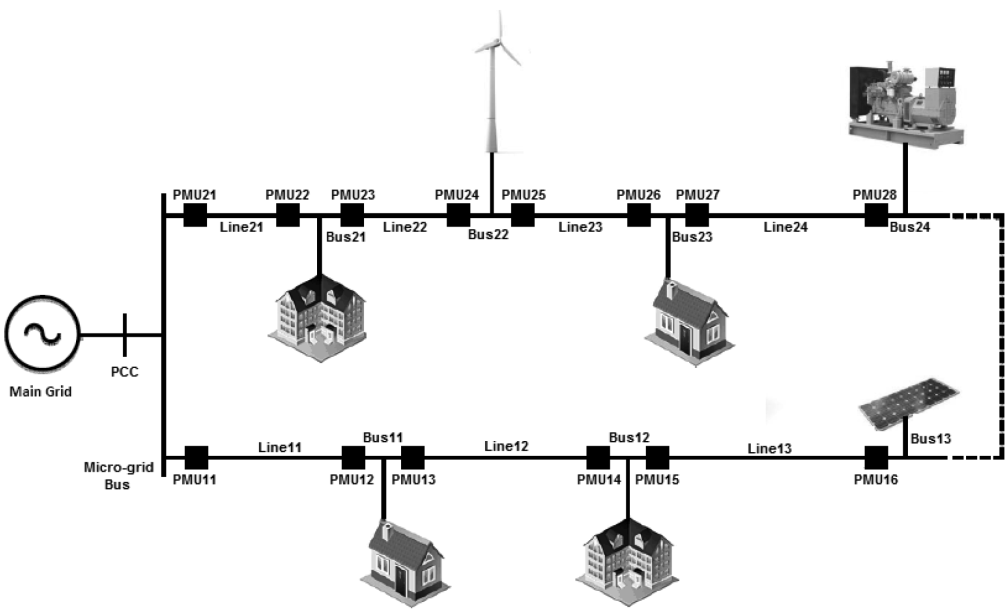

Figure 1. Structure of a typical micro-grid

The most significant advantage of micro-grid is that it can provide high-reliability and high-quality power for the customers who need uninterruptible power supplies. In addition, a significant cost saving comes from the application of Combined Heat and Power (CHP) systems in micro-grids. Notwithstanding numerous advantages provided by micro-grids, they may pose some technical challenges which need to be fulfilled for researchers. Micro-grid protection and its entities is one of them [11-13]. Protection of micro-grids cannot be attained by the same philosophies which have traditionally been applied in distribution networks. The reason is that a protection scheme for micro-grids should take the followings into account: (a) bidirectional power flow in feeders; (b) existence of looped feeders; (c) decreased magnitude of the fault current in stand-alone operation mode [14-16]. As a result, the traditional overcurrent-based protection strategies are ineffective for micro-grids and some alternative strategies should be employed.

In a study by Oudalov and Fidigatti [17], an adaptive protection strategy was suggested, applying digital relaying and advanced communication technique. In the presented technique, the protection settings were updated periodically by means of Micro-Grid Central Controller (MGCC) in accordance with micro-grid operating modes. However, the proposed strategy necessitated updating or upgrading the protection devices which are presently applied in the distribution networks; moreover, fault calculations were relatively sophisticated for a micro-grid functioning in different modes. Dewadasa and his research group [18, 19] proposed an additional methodology for inverter-based micro-grids. In their developed strategy, an admittance relay with inverse time tripping characteristics was designed. Despite the fact that the strategy had the ability to protect micro-grids either in grid-connected or in stand-alone mode, it was unable to protect micro-grids including rotating-based DERs. The further shortcoming of the strategy was that it was designed for only radial micro-grids. Tumilty et al. and Redfern and H. Al-Nasseri [20, 21] put forward a new protection approach based upon voltage measurements to protect autonomous micro-grids against different kinds of faults. Nevertheless, the suggested approach did not take account of grid-connected operating mode, High Impedance Faults (HIFs) as well as single-phase tripping. Jayawarna et al. [22, 23] proposed the installation of energy storage devices (such as batteries, flywheels, etc.) within the micro-grid to equalize the magnitude of short-circuit current in both grid-connected and stand-alone modes of operation. By the application of such devices, micro-grid could still be protected using conventional overcurrent-based protection, but required adaptive protective devices. The major drawback of the proposed strategy was that the cost pertaining to such devices with high short-circuit capacity was extremely disadvantageous. In a study by Sortomme et al. [24], a differential-based protection strategy was introduced which was able to protect micro-grids including radial or looped feeders in both modes of operation. However, the strategy was only effective for protection of lines and had not the ability to protect buses connected to DERs or loads. Nikkhajoei et al. [25] established an alternative protection method based upon symmetrical components. The authors applied zero- and negative-sequence currents to protect micro-grids against asymmetrical faults. However, the suggested technique was ineffective in detecting three-phase faults; besides, the capability of single-phase tripping had not been taken into account in the method. Subsequently, in a research by Zamani et al. [26] another protection strategy was devised using zero- and negative-sequence components which had the ability to protect micro-grids against different kinds of faults; also, the proposed strategy did not require communication system. The main problem associated with the proposed method was that it was to a large extent dependent on the network configuration, because the method had been designed for only radial micro-grids and was not capable of protecting micro-grids containing looped feeders; furthermore, due to the need for zero-sequence current in the proposed method, its implementation necessitated the application of specific types of transformers (only grounded transformers) inside the micro-grid.

This article presents a protection strategy for micro-grids using Phasor Measurement Units (PMUs) and a designed Microprocessor-Based Relaying (MBR) which can detect and isolate different kinds of faults in both grid-connected and islanded modes. The major feature of the developed strategy is that it is entirely independent of the micro-grid structure; furthermore, the capability of automatic updating of pick-up threshold value is taken into account in the designed MBR. Therefore, in the event of any change in the micro-grid configuration (such as disconnection of a line or a bus either in grid-connected mode or in islanded mode, transferring to the islanded mode of operation, as well as micro-grid expansion), the pick-up threshold value can be automatically readjusted according to the new structure.

The remainder of this article is organized as follows: next technical challenges in the protection of micro-grids are discussed; then the protection scheme is proposed; different parts of the designed MBR are introduced; simulation results using case studies are given; and finally, a conclusion is summarized.

TECHNICAL CHALLENGES IN THE PROTECTION OF MICRO-GRIDS

The majority of the distribution networks are designed to operate in radial mode, in which the power flows in one direction from higher voltage levels to lower voltage levels. Because of this, the protection of such networks is accomplished using simple and relatively low-cost overcurrent-based protective devices such as overcurrent relays, reclosers and fuses. When a micro-grid is formed in a distribution network, the configuration is changed to a complicated multi-source power system. The protection of micro-grid should be in such a way that a safe and secure protection is provided in both grid-connected and stand-alone operation modes [27, 28]. Nevertheless, the function of micro-grid in these two modes creates some new protection problems. During grid-connected operation mode, since micro-grid provides a large short-circuit current to the fault point, the protection can be performed by existing protective devices within the distribution networks, but in islanded mode, fault currents are drastically lower than those of grid-connected mode due to the presence of inverter-based DERs inside the micro-grids. The reason is that such types of DERs are designed to restrict their output current to approximately twice their rated current to protect their power devices. Hence, the employment of traditional overcurrent-based protective devices in micro-grids is no longer valid and some alternative protection schemes should be developed.

PROPOSED PROTECTION SCHEME

This article presents a protection scheme for micro-grids using PMUs and a designed MBR, thereby detecting different kinds of faults in both grid-connected and islanded modes of operation. In the proposed protection scheme, the PMUs which are responsible for extracting voltage and current phasors (magnitudes and their respective phasor angles) based upon digital sampling (at rates of at least 30 samples per second) of Alternating Current (AC) waveforms, are installed at both ends of each line of micro-grid. Subsequently, the information extracted by PMUs of each line is transferred to the MBR of that line through a digital communication system. Having occurred a fault within the micro-grid, the information received by PMUs in all MBRs is analyzed, and then the fault occurrence, location of fault, and faulted phases are recognized by the relevant MBR or MBRs. Subsequently, depending on the fault type, tripping signals are issued to the relevant circuit breakers.

Detection of Fault Incident

In case a fault takes place in a power network, it transfers from a balanced to an unbalanced status. In addition, because of the existence of single-phase DERs inside the micro-grids, they are inherently operated under unbalanced circumstances. As a result, presenting a method based upon symmetrical components can be considerably effective in differentiating between unbalanced and faulty conditions. Symmetrical components approach, developed by C.L. Fortescue, is one of the most effective ones which is applied to transform a three-phase unbalanced system into three sets of symmetrical balanced phasors, namely positive-, negative- and zero-sequence components. In case a fault strikes within a network, these symmetrical components are formed depending on the fault type. Table 1 illustrates the existence of symmetrical components during different types of faults. As can be seen from the table, the positive-sequence is the only component which exists in all types of faults. For this reason, in this study, the positive-sequence component is employed to detect different kinds of faults.

Table 1. Existence of symmetrical components during different types of faults

Fault Type	Positive-Sequence	Negative-Sequence	Zero-Sequence
Single Line to Ground	Yes	Yes	Yes
Line to Line	Yes	Yes	No
Line to Line to Ground	Yes	Yes	Yes
Three Phase	Yes	No	No

Detection of Fault Location

As mentioned earlier, the majority of the proposed methods to date are strongly dependent on the micro-grid configuration. In order to possess an appropriate method having the ability to protect different micro-grids with different configurations, micro-grid feeders should be sectionalized in such a way that each section (micro-grid's line or bus) is protected independent of other sections. To fulfill this, the upstream and downstream of each line are replaced with its upstream and downstream equivalent circuits, respectively. Both of these equivalent circuits include a voltage source in series with impedance. Figure 2 indicates the upstream and downstream equivalent circuits of Line 12 of Figure 1 during a fault.

Figure 2. Upstream and downstream equivalent circuits of Line 12 of Figure 1 during a fault

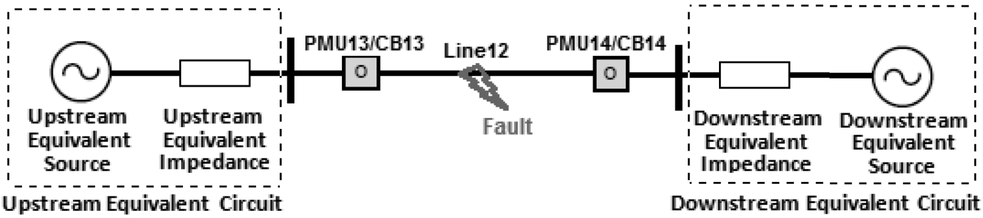

During a fault occurrence shown in Figure 2, different symmetrical components are created depending on the fault type. The equivalent circuit diagram in the system of symmetrical components for different kinds of faults by considering upstream and downstream equivalent circuits are depicted in Figure 3.

By replacing the equivalent impedance of negative- and zero-sequence networks between terminals AB of positive-sequence network for all types of faults, a general model for the analysis of different kinds of faults can be developed. The developed model is demonstrated in Figure 4, in which impedance $Z_{eq2,0}$ is the representative of negative- and zero-sequence networks.

Depending on the fault type, the value of the impedance is different. Equation 1 expresses the value of impedance $Z_{eq2,0}$,for different types of faults:

$$Z_{eq2,0} = \begin{cases} Z_{eq0} + Z_{eq2} & for\ single\ line\ to\ ground\ faults \\ Z_{eq2} & for\ line\ to\ line\ faults \\ Z_{eq0} \| Z_{eq2} & for\ line\ to\ line\ to\ ground\ faults \\ 0 & for\ three\ phase\ faults \end{cases} \quad (1)$$

where,

$Z_{eq0} = (Z_{U0} + Z_{LU0}) \| (Z_{D0} + Z_{LD0})$

$Z_{eq2} = (Z_{U2} + Z_{LU2}) \| (Z_{D2} + Z_{LD2})$

In the proposed protection scheme, after the detection of fault incident, the faulted section is recognized by the developed model of Figure 4 in such a way as to compare the value of upstream and downstream

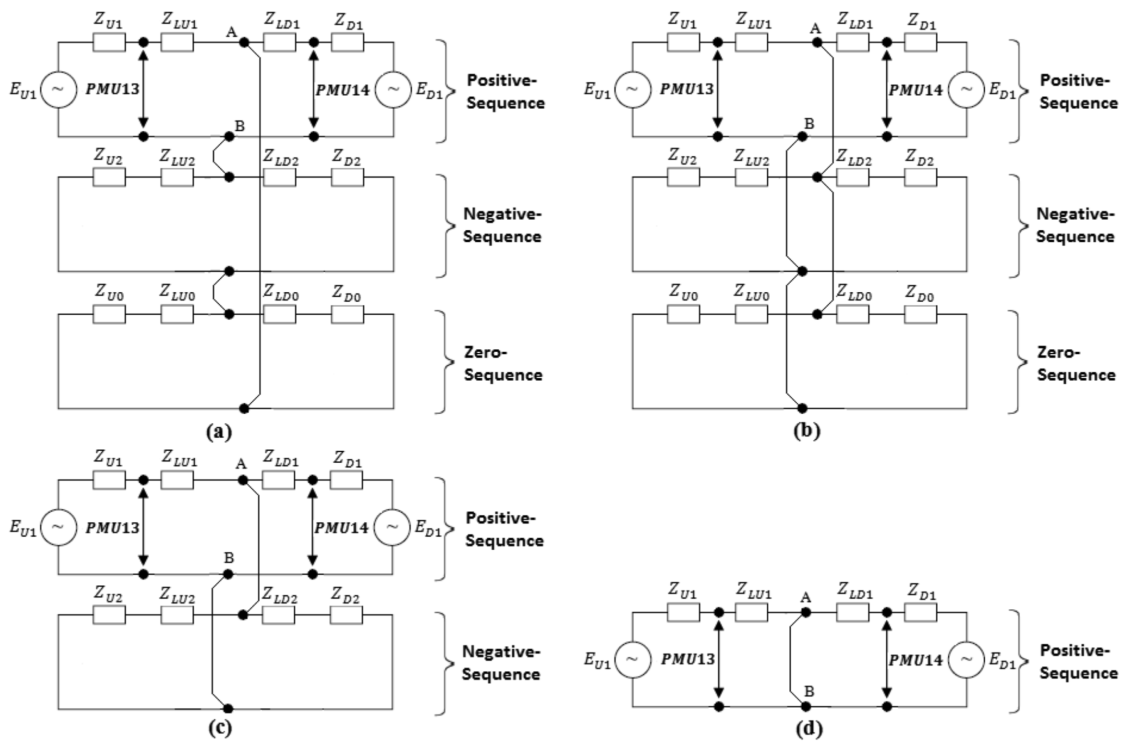

Figure 3. Equivalent circuit diagram in the system of symmetrical components by considering upstream and downstream equivalent circuits for: (a) Single line to ground fault, (b) Line to line to ground fault, (c) Line to line fault, (d) Three phase fault

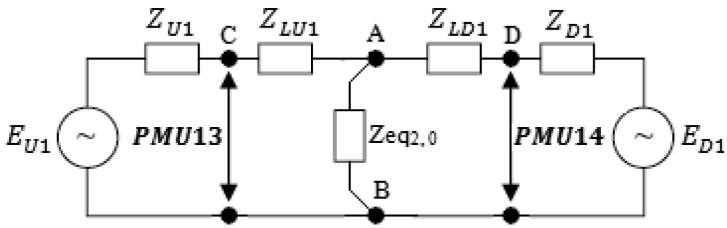

Figure 4. Developed general model for the analysis of different kinds of faults

equivalent positive-sequence impedances, before and after the fault. In fact, when a fault occurs inside a line, impedance $Z_{eq2,0}$ is created between points C and D. Therefore, the values of both upstream and downstream equivalent positive-sequence impedances after the fault (Z_{U1}, Z_{D1}) remain equal to the values of those impedances before the fault $Z_{U1\,(pre)}$, $Z_{D1\,(pre)}$, but in case a fault occurs at the upstream or downstream of a line, respectively, only the value of Z_{D1},or only the value of Z_{U1} remains constant after the fault.

Figure 5 depicts the single-phase diagram of the proposed protection scheme for Line 12 and its adjacent buses in the micro-grid shown in Figure 1. As can be seen in the figure, MBR_Line12 has three outputs for each phase. When a fault occurs inside of Line12, the values of both (Z_{U1}, Z_{D1}) remain constant; in fact, both PMU13 and PMU14 see the fault in their forward side, so the Line12 Fault Trip signal is issued to both CB13 and CB14, but in case a fault occurs at Bus11, the values of Z_{D1} from MBR_Line12 and Z_{U1} from MBR_Line11 remain constant, so PMU12 and PMU13 Reverse Fault Trip signals are issued respectively from MBR_ Line11 and MBR_Line12, and disconnect CB12 and CB13. Similarly, in case of a fault incident at Bus12, PMU14 and PMU15 Reverse Fault Trip signals are issued respectively from MBR_Line12 and MBR_Line13, and disconnect CB14 and CB15.

DESIGNED MICROPROCESSOR-BASED RELAY (MBR)

Figure 6 displays the schematic diagram of MBR_Line12. As can be seen in the figure, it consists of four main parts, namely, fault incident detector, fault locator, faulty phase detector and blocking signal issue-maker, each of which are described in detail in the following subsections.

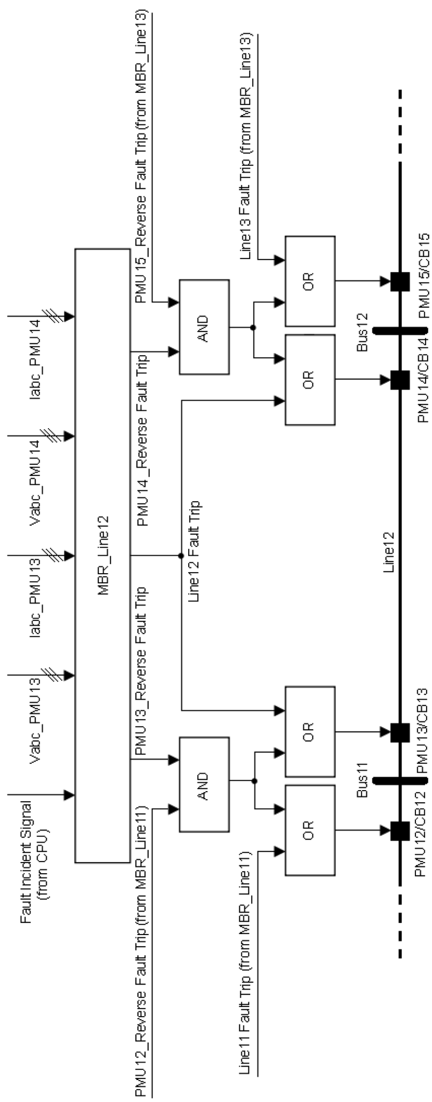

Figure 5. Single-phase diagram of the proposed protection scheme for Line 12 and its adjacent buses in the micro-grid shown in Figure 1

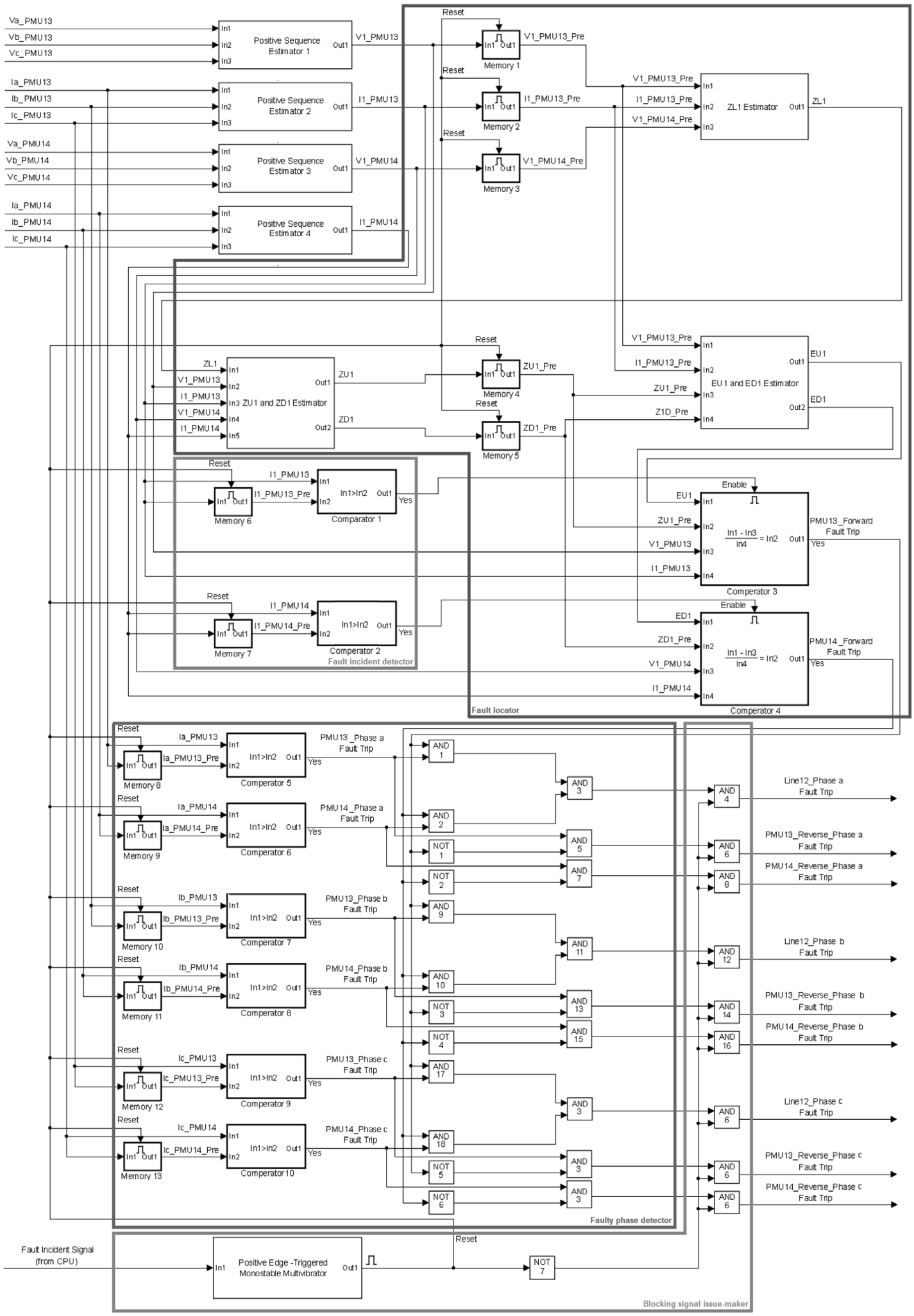

Figure 6. Schematic diagram of MBR_Line12

Fault Incident Detector

As explained earlier, the positive-sequence component is the only component which exists in all types of faults. Therefore, in the proposed protection scheme, the component is used to detect different kinds of faults. When a fault occurs in a section, the positive-sequence current magnitude of that section is increased; hence, the fault occurrence can be detected by comparing the magnitude before and after the fault. In the designed MBR, for the detection of fault in each section, a fault incident detector is allocated. However, as a fault in one section may increase the positive-sequence current magnitude of other sections, the MBRs of other lines may issue fault trip signals and therefore CBs of several sections are disconnected. Hence, a fault locator is also considered in the designed MBR.

Fault Locator

As mentioned in Subsection 3.2, the faulted section is identified based on changes in the values of upstream and downstream equivalent positive-sequence impedances before and after the fault. In the designed MBR, this function is performed by fault locator. Prior to fault incident, the fault locator, first, calculates the values of Thevenin's Equivalent Positive-Sequence Impedances (TEPSIs) at both ends of each section, and then it deploys the values to determine the values of impedances $Z_{U1\,(pre)}$ and $Z_{D1\,(pre)}$.

Finally, the faulted section can be recognized by comparing the values of upstream and downstream equivalent positive-sequence impedances before $Z_{U1\,(pre)}$, $Z_{D1\,(pre)}$ and after Z_{U1} Z_{D1} the fault.

In order to determine the TEPSI of each point within the micro-grid, this article introduces an online methodology by using three consecutive voltage and current measurements of PMUs at different time instants. Since any changes in the frequency of the micro-grid system will lead to slip between micro-grid frequency system and the PMU sampling frequency, phase angles of voltage and current for these three measurements will be different.

Figure 7 illustrates the equivalent circuit diagram of the positive-sequence network for Line 12 (of Figure 1) prior to fault occurrence.

The positive-sequence voltage equation for PMU13 terminals using Thevenin's model is as follows:

$$V_{1PMU13} = E_{t1PMU13} + Z_{t1PMU13} \bullet I_{1PMU13} \tag{2}$$

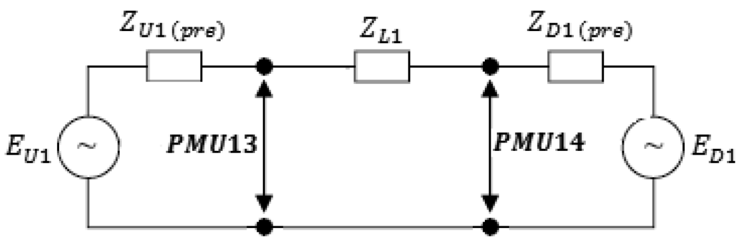

Figure 7. Equivalent circuit diagram of the positive-sequence network for Line 12 (of Figure 1) prior to fault occurrence

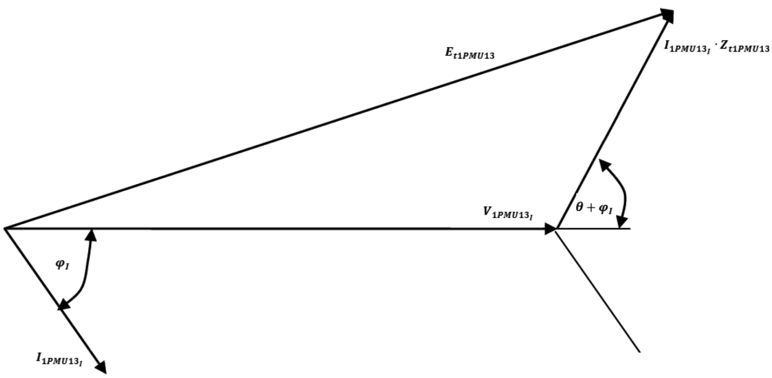

(**a**)

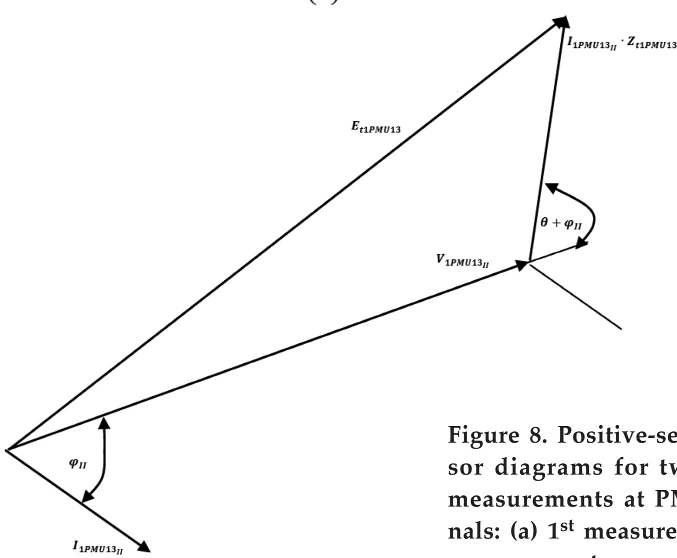

(**b**)

Figure 8. Positive-sequence phasor diagrams for two different measurements at PMU13 terminals: (a) 1st measurement (b) 2nd measurement

where,

$E_{t1PMU13}$ = Thevenin's equivalent positive-sequence voltage source at PMU13 terminals

$Z_{t1PMU13}$ = Thevenin's equivalent positive-sequence impedance at PMU13 terminals

Positive-sequence phasor diagrams of Equation (2) for two different measurements at PMU13 terminals are indicated in Figure 8.

Since $E_{t1PMU13}$ is the Thevenin's positive-sequence equivalent voltage source, its magnitude for both measurements are identical, but its angle in the 2nd measurement is shifted by an angle equal to the phase drift. Referring to Figure 8, $E_{t1PMU13}$ equation for the 1st measurement can be written as:

$$E_{t1PMU13}^2 = V_{1PMU13_I}^2 + I_{1PMU13_I}^2 \cdot Z_{t1PMU13}^2 + 2V_{1PMU13_I} \cdot I_{1PMU13_I} \cdot Z_{t1PMU13} \cdot \cos(\theta + \varphi_I) \quad (3)$$

By expanding, cos ($\theta + \varphi_{11}$), Equation (3) can be expressed as follows:

$$E_{t1PMU13}^2 = V_{1PMU13_I}^2 + I_{1PMU13_I}^2 \cdot Z_{t1PMU13}^2 + 2P_{1PMU13_I} \cdot R_{t1PMU13} - 2Q_{1PMU13_I} \cdot X_{t1PMU13} \quad (4)$$

Where $R_{t1PMU13}$ and $X_{t1PMU13}$ denote the resistance and reactance of the Thevenin's equivalent positive-sequence impedance, as well as P_{1PMU13_1} and Q_{1PMU13_1}, which respectively represent active and reactive powers flowing through Line 12. Likewise, the $E_{t1PMU13}$ equation for the 2nd measurement can be written as:

$$E_{t1PMU13}^2 = V_{1PMU13_{II}}^2 + I_{1PMU13_{II}}^2 \cdot Z_{t1PMU13}^2 + 2P_{1PMU13_{II}} \cdot R_{t1PMU13} - 2Q_{1PMU13_{II}} \cdot X_{t1PMU13} \quad (5)$$

By subtracting Equation (5) from Equation (4):

$$V_{1PMU13_I}^2 - V_{1PMU13_{II}}^2 + \left(I_{1PMU13_I}^2 - I_{1PMU13_{II}}^2\right) \cdot Z_{t1PMU13}^2 + 2\left(P_{1PMU13_I} - P_{1PMU13_{II}}\right) \cdot R_{t1PMU13} - 2(Q_{1PMU13_I} - Q_{1PMU13_{II}}) \cdot X_{t1PMU13} = 0 \quad (6)$$

Equation (6) can be arranged as follows:

$$\left(R_{t1PMU13}+\frac{P_{1PMU13_I}-P_{1PMU13_{II}}}{I^2_{1PMU13_I}-I^2_{1PMU13_{II}}}\right)^2+\left(X_{t1PMU13}-\frac{Q_{1PMU13_I}-Q_{1PMU13_{II}}}{I^2_{1PMU13_I}-I^2_{1PMU13_{II}}}\right)^2=$$
$$\frac{V^2_{1PMU13_{II}}-V^2_{1PMU13_I}}{I^2_{1PMU13_I}-I^2_{1PMU13_{II}}}+\left(\frac{P_{1PMU13_I}-P_{1PMU13_{II}}}{I^2_{1PMU13_I}-I^2_{1PMU13_{II}}}\right)^2+\left(\frac{Q_{1PMU13_I}-Q_{1PMU13_{II}}}{I^2_{1PMU13_I}-I^2_{1PMU13_{II}}}\right)^2 \quad (7)$$

This is the equation of a circle in the positive-sequence impedance plane which indicates a locus for the Thevenin's equivalent positive-sequence impedance seen from PMU13 terminals. As it does not specify a certain value for $Z_{t1PMU13}$, a third measurement is required so that it is used with the first and second measurements to create another two circles for $Z_{t1PMU13}$. Figure 9 shows the positive-sequence impedance plane including the circles obtained from three different measurements. As shown in Figure 9, the value of Thevenin's equivalent positive-sequence impedance seen from PMU13 terminals is specified by the intersection of the three circles.

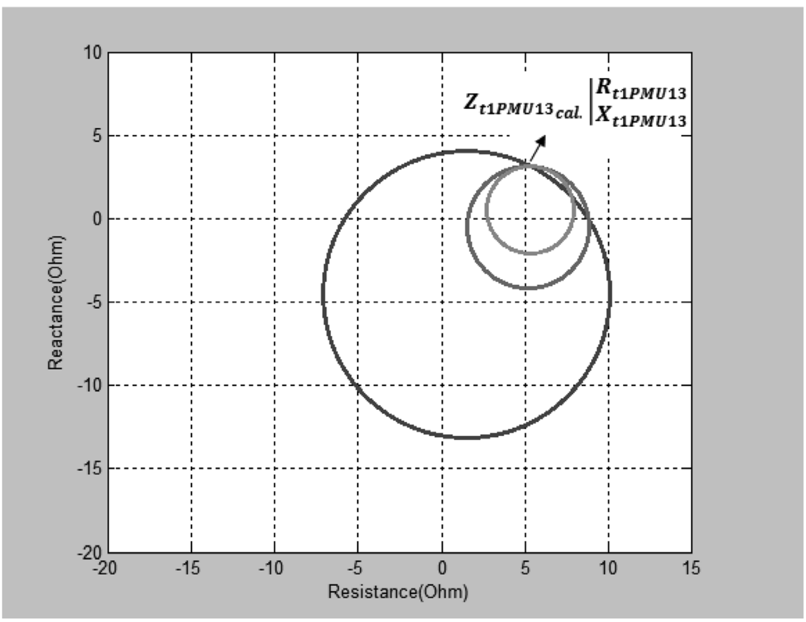

Figure 9. Positive-sequence impedance plane including the circles obtained from three different measurements

According to Thevenin's theorem, Thevenin's equivalent impedance for any two-terminal of the network is the impedance seen from those terminals when the sources are set to zero. Hence, $Z_{t1PMU13}$ for PMU13 terminals of Figure 7 is equivalent to ZU1||(ZL1 + ZD1). By setting this equal to the calculated Zt1PMU13 from the intersection point of the three circles:

$$\text{Zt1PMU13}_{\text{cal.}} = \text{ZU1(pre)}||(\text{ZL1} + \text{ZD1(pre)}) \quad (8)$$

By following the same procedure for PMU14 terminals of Figure 7:

$$\text{Zt1PMU14}_{\text{cal.}} = \text{ZD1(pre)}||(\text{ZL1} + \text{ZU1(pre)}) \quad (9)$$

By solving Equations (8) and (9), the values of ZU1(pre) and ZD1(pre) are obtained. Subsequently, fault locators related to each section compare the values of ZU1(pre) and ZD1(pre) with the values of ZU1 and ZD1 after the fault incident and identify the faulted section.

Faulty Phase Detector

Single-phase tripping capability has long been regarded as an effective way of improving system security and reliability. It leads to removal of unnecessary interruptions of the unaffected phases in case the fault does not involve all three phases. In the designed MBR, having detected the faulted section by means of the fault locator, the affected phases of that section are identified through faulty phase detector. The faulty phase detector compares the positive-sequence current magnitude of each phase of the faulted section before and after the fault, and then issues the proper disconnection signals to the relevant circuit breakers of that section.

Blocking Signal Issue-maker

In order to update the values of ZU1(pre) and ZD1(pre) as well as precluding from mal-operation of MBRs for the second fault, a blocking signal issue-maker has been considered in designing the MBRs. In fact, after the isolation of the first fault (inside or outside of micro-grid), a Fault Incident signal is issued from the Central Protection Unit (CPU) to all MBRs. The signal is responsible for resetting the memories as well as blocking the outputs of all MBRs within the micro-grid until the new values of ZU1(pre) and ZD1(pre) are determined. To fulfill this, a Positive Edge-Triggered Monostable Multivibrator is used. Once it received a Fault Incident signal resulted from the disconnection of CBs within the micro-grid, generates an output pulse with the duration of T. It is clear that the duration of the pulse should be more than the time which is needed so that the values of ZU1(pre) and ZD1(pre) are updated.

SIMULATION RESULTS

In order to evaluate the effectiveness of the proposed scheme and the designed MBR, several simulations have been carried out by using DIgSILENT PowerFactory and Matlab software packages. The configuration of the simulated micro-grid which, hereinafter is referred to as "study micro-grid" as well as the case studies are presented in the following subsections.

Study Micro-grid

The single-line diagram of the study micro-grid is illustrated in Figure 10. As can be seen in the figure, the study micro-grid is connected to the main grid by means of a 69kV/24.9kV Dyn transformer. It also includes two photovoltaic parks and one wind farm which are interfaced with the network through respective YNyn transformers. The information associated with the applied transformers, DER units, loads, cables, as well as the configuration of conductors of the study micro-grid are listed in Tables 2 to 6.

Case Studies

To prove the efficacy of the designed MBR in the grid-connected and islanded operating modes, several MBRs have been simulated, but due to space restriction and format requirements of this publication, only the simulation results of MBR_Line203 is included in this article. According to the simulation results, the calculated values of upstream and downstream equivalent positive-sequence impedances (from intersection of circles) for Line 203 before the fault incidents in both grid-connected and islanded operating modes are as follows:

$$Z_{U1\,L203\,(pre)_{cal.}} = \begin{cases} 8.7424\ (\Omega) & for\ grid-connected\ mode \\ 11.1013\ (\Omega) & for\ islanded\ mode \end{cases}$$

$$Z_{D1\,L203\,(pre)_{cal.}} = \begin{cases} 8.5436\ (\Omega) & for\ grid-connected\ mode \\ 10.8321\ (\Omega) & for\ islanded\ mode \end{cases}$$

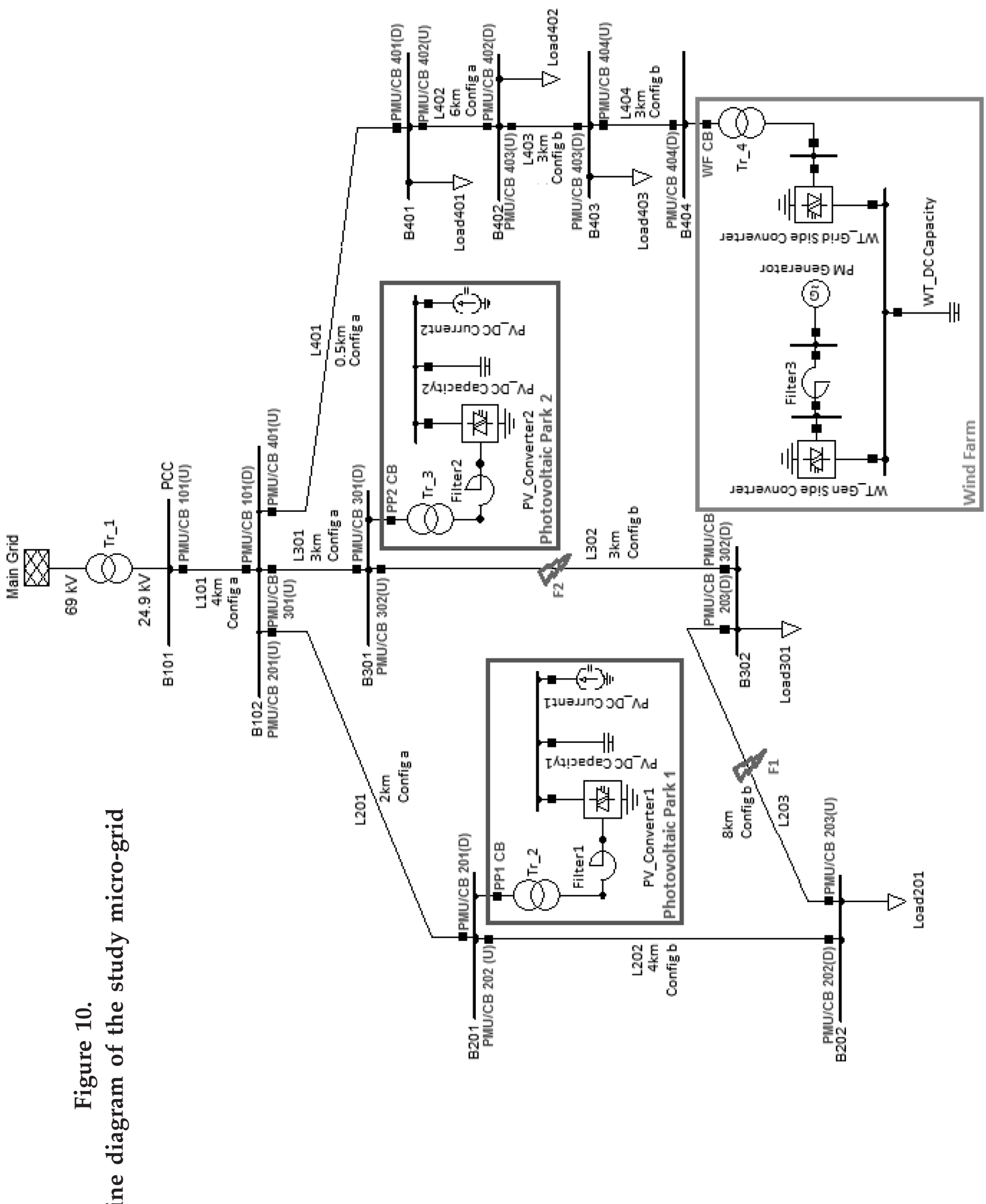

Figure 10.
Single-line diagram of the study micro-grid

Table 2. The information associated with the applied transformers in the study micro-grid

Transformer Type	HV (kV)	LV (kV)	Rated Power	UK %	X/R Ratio	Vector Group
Tr-1	69	24.9	2	3	8	Dyn0
Tr-2	24.9	0.4	5	11	2.1474	YNyn0
Tr-3	24.9	0.4	5	11	2.1474	YNyn0
Tr-4	24.9	0.4	5	11	2.1474	YNyn0

Table 3. The information associated with the applied DER units in the study micro-grid

Generation Units' Components	Nominal Voltage (kV)	Nominal Current (A)	Rated Apparent Power (MVA)
PM Generator	0.4	-	1
PV_DC Current1	-	1	-
PV_DC Current1	-	1	-
PV_DC Capacity1	1	-	-
PV_DC Capacity1	1	-	-

Table 4. The information associated with the loads in the study micro-grid

Name	Phase A		Phase B		Phase C	
	kW	kVAR	kW	kVAR	kW	kVAR
Load201	100	16	75	14	30	3
Load301	175	22	53	18	10	2
Load401	14	5	77	13	21	7
Load402	93	26	24	10	18	5
Load403	111	38	28	3	12	6

Table 5. The information associated with the cables in the study micro-grid

Conductor Type	Nominal Current (kA)	DC Resistance (ohm/km)	GMR (mm)	Outer Diameter (mm)
# 1ACSR	0.23	0.695936	1.359408	10.1092
# 2ACSR	0.18	1.050117	1.274064	8.127999

where,
$ZU1L203(pre)_{cal}$ = Upstream equivalent positive-sequence impedance of PMU203 (U)

$ZD1L203(pre)_{cal}$ = Downstream equivalent positive-sequence impedance of PMU203 (D)

Tables 7 and 8 indicate the simulation results of MBR_Line203 during different kinds of faults at the midpoint of Lines 203 and 302 (F1 and F2 in Figure 10) in both grid-connected and islanded operating modes, respectively.

CONCLUSION

This article proposed a novel protection strategy using positive-sequence component for micro-grids. The proposed strategy which addresses the protection issues of a micro-grid in both modes of operation can be implemented through PMUs, a designed MBR and a narrowband communication system. The salient feature of the proposed protection strategy is that it does not depend on the micro-grid configuration and can be applied for micro-grids including radial and looped feeders. It also has the ability to automatically update the pick-up threshold value. Furthermore, the proposed strategy enables single-phase tripping to increase security of supply. Lastly, in order to demonstrate the efficacy of the proposed protection scheme and the designed MBR, several simulations were accomplished by using DIgSILENT PowerFactory and Matlab software packages.

References

1. P.S. Georgilakis and N.D. Hatziargyriou, Optimal distributed generation placement in power distribution networks: models, methods, and future research, IEEE Transactions on Power Systems, 28(3), 3420-3428, 2013, DOI: 10.1109/TP-

Table 6. Configuration of conductors of the study micro-grid

Tower Type	R_ij (Ohm/km)			X_ij (Ohm/km)			B_ij (uS/km)			Conductor
Config a	0.1323521	0.1305501	0.830649	0.3116177	0.3590904	0.8290956	-0.6178294	-0.9515057	3.315015	# 1ACSR
	0.1283753	0.8225712	0.1305501	0.2852715	0.8431386	0.3590904	-0.3859958	3.167688	-0.9515057	
	0.8260509	0.1283753	0.1323521	0.8370491	0.2852715	0.3116177	3.037262	-0.3859958	-0.6178294	
Config b	0.1465815	0.1445931	1.199246	0.3536223	0.4002873	0.8770654	-0.5842132	-0.8925376	3.181855	# 2ACSR
	0.1421697	1.190361	0.1445931	0.3254742	0.8873802	0.4002873	-0.369778	3.048136	-0.8925376	
	1.194213	0.1421697	0.1465815	0.8829063	0.3254742	0.3536223	2.930014	-0.369778	-0.5842132	

Table 7. Simulation results of MBR_Line203 during different kinds of faults at the midpoint of Lines 203 and 302 (F1 and F2 in Figure 10) in the grid-connected operating mode

Fault Type		AG		BC		BCG		ABC	
Fault Location		F1	F2	F1	F2	F1	F2	F1	F2
PMU203 (U)	$\lvert\vec{V}_{1PMU203\,(U)}\rvert$ (kV)	11.5966	11.9350	9.6348	10.3793	8.4334	9.3542	5.5298	7.0634
	$\lvert\vec{E}_{U1}-\vec{V}_{1PMU203\,(U)}\rvert$ (kV)	2.7971	2.4659	4.7554	4.0319	5.9731	5.0408	8.8869	7.3347
	$\lvert\vec{I}_{1PMU203\,(U)}\rvert$ (A)	321.5102	282.7916	545.9724	460.7890	683.4320	578.0777	1015.652	840.1829
	$\lvert\vec{I}_{APMU203\,(U)}\rvert$ (A)	965.496	815.6665	1.5572	5.6577	1.4117	29.6650	1013.2202	842.7955
	$\lvert\vec{I}_{BPMU203\,(U)}\rvert$ (A)	2.0832	35.9602	944.5889	794.6007	1004.1611	843.5396	1032.0512	849.6995
	$\lvert\vec{I}_{CPMU203\,(U)}\rvert$ (A)	1.7248	37.2584	945.2113	796.4882	1056.3031	872.4384	1001.9256	830.1382
PMU203 (D)	$\lvert\vec{V}_{1PMU203\,(D)}\rvert$ (kV)	11.6082	10.7275	9.6623	8.0940	8.4671	6.4597	5.5934	2.4528
	$\lvert\vec{E}_{D1}-\vec{V}_{1PMU203\,(D)}\rvert$ (kV)	2.7872	3.6819	4.7308	6.3265	5.9364	8.0298	8.8155	11.9826
	$\lvert\vec{I}_{1PMU203\,(D)}\rvert$ (A)	326.7549	489.6217	554.6120	863.8151	693.5113	1118.3574	1031.0640	1756.9881
	$\lvert\vec{I}_{APMU203\,(D)}\rvert$ (A)	980.0686	1410.6070	1.6165	10.2899	1.1747	58.6042	1028.2876	1760.8619
	$\lvert\vec{I}_{BPMU203\,(D)}\rvert$ (A)	1.8584	63.1623	962.1998	1488.0535	1020.62	1630.9718	1050.3911	1775.9912
	$\lvert\vec{I}_{CPMU203\,(D)}\rvert$ (A)	1.8134	64.4086	963.5132	1484.2312	1070.2334	1687.0680	1015.5264	1733.9268
$Z_{U1\,L203}=\frac{\lvert\vec{E}_{U1}-\vec{V}_{1PMU203\,(U)}\rvert}{\lvert\vec{I}_{1PMU203\,(U)}\rvert}$ (Ω)		≅ 8.7427	≅ 8.7427	≅ 8.7427	≅ 8.7427	≅ 8.7427	≅ 8.7427	≅ 8.7427	≅ 8.7427
$Z_{D1\,L203}=\frac{\lvert\vec{E}_{D1}-\vec{V}_{1PMU203\,(D)}\rvert}{\lvert\vec{I}_{1PMU203\,(D)}\rvert}$ (Ω)		≅ 8.5436	≠ 8.5436	≅ 8.5436	≠ 8.5436	≅ 8.5436	≠ 8.5436	≅ 8.5436	≠ 8.5436
Operated CBs in Line 203	Phase A	Yes	No	No	No	No	No	Yes	No
	Phase B	No	No	Yes	No	Yes	No	Yes	No
	Phase C	No	No	Yes	No	Yes	No	Yes	No

Table 8. Simulation results of MBR_Line203 during different kinds of faults at the midpoint of Lines 203 and 302 (F1 and F2 in Figure 10) in the islanded operating mode

Fault Type		AG		BC		BCG		ABC	
Fault Location		F1	F2	F1	F2	F1	F2	F1	F2
PMU203 (U)	$\lvert\vec{V}_{1PMU203\,(U)}\rvert$ (kV)	11.0988	11.3099	9.1148	9.7430	7.7168	8.4308	4.7300	5.9963
	$\lvert\vec{E}_{U1}-\vec{V}_{1PMU203\,(U)}\rvert$ (kV)	3.2179	2.9887	5.1640	4.5415	6.5494	5.8419	9.5093	8.2544
	$\lvert\vec{I}_{1PMU203\,(U)}\rvert$ (A)	290.7223	271.7043	469.4610	412.8664	595.4070	531.0826	864.488	750.407
	$\lvert\vec{I}_{APMU203\,(U)}\rvert$ (A)	871.7310	780.5351	283.8310	6.1624	1.3531	32.8874	864.2287	752.7404
	$\lvert\vec{I}_{BPMU203\,(U)}\rvert$ (A)	1.9033	37.2396	812.2162	711.8386	901.8585	787.9563	873.3966	755.1645
	$\lvert\vec{I}_{CPMU203\,(U)}\rvert$ (A)	2.7320	38.5795	813.0602	714.4253	887.0783	774.6245	856.5223	743.8610
PMU203 (D)	$\lvert\vec{V}_{1PMU203\,(D)}\rvert$ (kV)	11.1005	10.1237	9.1258	7.9855	7.7301	6.0760	4.7564	2.3284
	$\lvert\vec{E}_{D1}-\vec{V}_{1PMU203\,(D)}\rvert$ (kV)	3.2345	4.2114	5.2147	6.3656	6.6143	8.2511	9.5962	12.0032
	$\lvert\vec{I}_{1PMU203\,(D)}\rvert$ (A)	298.6682	427.9913	481.5108	659.6570	610.7423	876.8526	886.0849	1303.2842
	$\lvert\vec{I}_{APMU203\,(D)}\rvert$ (A)	897.4405	1227.3911	1.7442	9.6282	1.3559	55.3565	885.1997	1307.2058
	$\lvert\vec{I}_{BPMU203\,(D)}\rvert$ (A)	1.9016	59.4333	835.5210	1138.5775	927.1934	1300.3894	897.0286	1311.4149
	$\lvert\vec{I}_{CPMU203\,(D)}\rvert$ (A)	2.8783	60.6821	834.5074	1140.6830	909.2486	1278.7700	876.2706	1291.6592
$Z_{U1\,L203}=\frac{\lvert\vec{E}_{U1}-\vec{V}_{1PMU203\,(U)}\rvert}{\lvert\vec{I}_{1PMU203\,(U)}\rvert}$ (Ω)		≅ 11.1013	≅ 11.1013	≅ 11.1013	≅ 11.1013	≅ 11.1013	≅ 11.1013	≅ 11.1013	≅ 11.1013
$Z_{D1\,L203}=\frac{\lvert\vec{E}_{D1}-\vec{V}_{1PMU203\,(D)}\rvert}{\lvert\vec{I}_{1PMU203\,(D)}\rvert}$ (Ω)		≅ 10.8321	≠ 10.8321	≅ 10.8321	≠ 10.8321	≅ 10.8321	≠ 10.8321	≅ 10.8321	≠ 10.8321
Operated CBs in Line 203	Phase A	Yes	No	No	No	No	No	Yes	No
	Phase B	No	No	Yes	No	Yes	No	Yes	No
	Phase C	No	No	Yes	No	Yes	No	Yes	No

10% Online Discount
Use Code JR10

EXPLORING THE VALUE OF ELECTRICITY

Clark W. Gellings

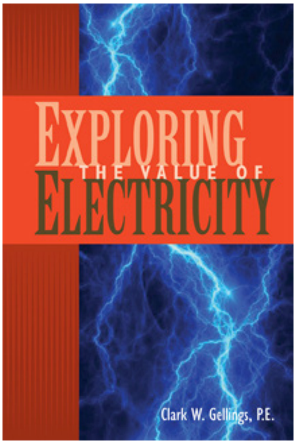

Intended for electric utility managers, directors, R&D and power system planners, economists, energy engineers, electrical manufacturers, and others involved in the field, this first-of-its-kind book provides an in-depth look at both the hard facts and some of the falsehoods about measuring the value of electricity. Coalescing the many wide ranging and disparate value estimates, it examines how we might better quantify the significance of avenues by which electricity plays a role in sustaining and improving the quality of life - i.e., via warmth, illumination, transportation, motive power, medical diagnostics, and life-prolonging treatments. The author elucidates the numerous approaches to estimating value, including electricity's contribution toward the U.S. gross domestic product, its role in medicine, and its ability to power communications. Traditional measures such the cost of outages, the impact of storms, the cost of restoring power systems after storms, the value of lost load (VOLL), consumer willingness to pay to avoid outages, and consumer surveys are also discussed.

ISBN: 0-88173-748-8

6 x 9, 254 pp., Illus., Hardcover

$110
ORDER CODE: 0708

CONTENTS

BOOK ORDER FORM

① Complete quantity and amount due for each book you wish to order:

Quantity	Book Title	Order Code	Price	Amount Due
	Exploring the Value of Electricity	**0708**	**$110.00**	
			Applicable Discount	
			Georgia Residents add 6% Sales Tax	
			Shipping $10 first book $4 each additional book	**10.00**
			TOTAL	

② Indicate shipping address: CODE: Journal 2014

NAME (Please print) BUSINESS PHONE

SIGNATURE (Required to process order) EMAIL ADDRESS

COMPANY

STREET ADDRESS ONLY (No P.O. Box)

CITY, STATE, ZIP

③ Select method of payment:
☐ **CHECK ENCLOSED**
☐ **CHARGE TO MY CREDIT CARD**
☐ *VISA* ☐ *MASTERCARD* ☐ *AMERICAN EXPRESS*

Make check payable in U.S. funds to:
AEE ENERGY BOOKS

CARD NO.

Expiration date *Signature*

MEMBER DISCOUNTS—A 15% discount is allowed to AEE members (discounts cannot be combined).
☐ **AEE Member (Member No.______________)**

④ Send your order to:
AEE BOOKS
P.O. Box 1026
Lilburn, GA 30048

INTERNET ORDERING
www.aeecenter.org/books
(use discount code)

TO ORDER BY PHONE
Use your credit card and call:
(770) 925-9558

TO ORDER BY FAX
Complete and Fax to:
(770) 381-9865

INTERNATIONAL ORDERS
Must be prepaid in U.S. dollars and must include an additional charge of $10.00 per book plus 15% for shipping and handling by surface mail.

10% Online Discount
Use Code JR10

GUIDE TO ENERGY MANAGEMENT 8th Edition

Barney L. Capehart
Wayne C. Turner, and William J. Kennedy

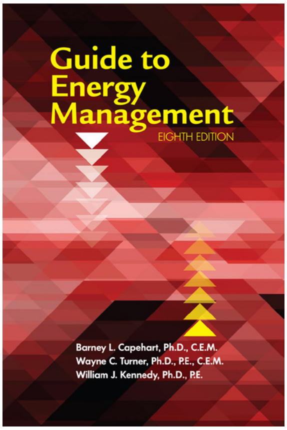

Completely revised and edited throughout, the latest edition of this best-selling reference includes four new chapters covering electrical distribution systems; motors and drives; building commissioning; and the impact of human behavior on facility energy management. Also updated are chapters on lighting, HVAC systems, web based building automation and control systems, green buildings, and greenhouse gas management. Written by three of the most respected energy professionals in the industry, this book examines the fundamental objectives of energy management, and illustrates techniques and tools proven effective for achieving results. Guide to Energy Management continues as one of the leading educational resources, both for individuals who are currently active as an energy managers or energy professionals, as well as for those just entering the field. It is the most widely used college and university textbook on the topic, as well as one of the most extensively used books for professional development training in the field, with well over 17,000 energy professionals having used it as a part of their training. Additional topics covered include energy auditing, energy bills, life cycle costing, electrical distribution systems, boilers, steam distribution systems, control systems and computers, energy systems maintenance, insulation, compressed air, renewable energy sources and water management, distributed generation and creating green buildings.

ISBN: 0-88173-765-8

6 x 9, 749 pp., Illus., Hardcover

Non-Member Price: $145.00
Order Code: 0714

CONTENTS

BOOK ORDER FORM

① Complete quantity and amount due for each book you wish to order:

Quantity	Book Title	Order Code	Price	Amount Due
	GUIDE TO ENERGY MANAGEMENT, 8th Edition	**0714**	**$145.00**	
			Applicable Discount	
			Georgia Residents add 6% Sales Tax	
			Shipping $10 first book $4 each additional book	**10.00**
			TOTAL	

② Indicate shipping address: CODE: Journal 2016

NAME (Please print) BUSINESS PHONE

SIGNATURE (Required to process order) EMAIL ADDRESS

COMPANY

STREET ADDRESS ONLY (No P.O. Box)

CITY, STATE, ZIP

MEMBER DISCOUNTS—A 15% discount is allowed to AEE members (discounts cannot be combined).
☐ **AEE Member (Member No.________________)**

③ Select method of payment:
☐ **CHECK ENCLOSED**
☐ **CHARGE TO MY CREDIT CARD**
☐ *VISA* ☐ *MASTERCARD* ☐ *AMERICAN EXPRESS*

Make check payable in U.S. funds to:
AEE ENERGY BOOKS

CARD NO.

Expiration date *Signature*

④ Send your order to:
AEE BOOKS
P.O. Box 1026
Lilburn, GA 30048

INTERNET ORDERING
www.aeecenter.org/books
(use discount code)

TO ORDER BY PHONE
Use your credit card and call:
(770) 925-9558

TO ORDER BY FAX
Complete and Fax to:
(770) 381-9865

INTERNATIONAL ORDERS
Must be prepaid in U.S. dollars and must include an additional charge of $10.00 per book plus 15% for shipping and handling by surface mail.

WRS.2012.2237043.

2. M.B. Delghavi and A. Yazdani, A control strategy for islanded operation of a distributed resource (DR) unit, in Proc. IEEE Power Energy Soc. Gen. Meeting, 1-8, 2009, DOI: 10.1109/PES.2009.5275592.
3. H. Nikkhajoei and R.H. Lasseter, Distributed generation interface to the CERTS microgrid, IEEE Transactions on Power Delivery, 24(3), 1598-1608, 2009, DOI: 10.1109/TPWRD.2009.2021040.
4. A. Baziar and A. Kavousi Fard, Considering uncertainty in the optimal energy management of renewable micro-grids including storage devices, Renewable Energy, 59, 158-166, 2013, DOI: [1]10.1016/j.renene.2013.03.026.M.P. Nthontho, S.P. Chowdhury, S. Winberg and S. Chowdhury, Protection of domestic solar photovoltaic based microgrid. in Proceedings of the 11th International Conference on Developments in Power Systems Protection, Birmingham, 1-6, 2012.
5. X. Li, A. Dysko and G.M. Burt, Application of communication based distribution protection schemes in islanded systems. in Proceedings of the14th International Universities Power Engineering Conference(UPEC), Cardiff, 1-6, 2010.
6. M.A. Zamani, A. Yazdani and T.S. Sidhu, A communication-assisted protection strategy for inverter-based medium-voltage microgrids, IEEE Transactions on Smart Grid, 3, 2088-2099, 2012, DOI: 10.1109/TSG.2012.2211045.
7. S. Mirsaeidi, D. Mat Said, M. Wazir Mustafa, M. Hafiz Habibuddin and K. Ghaffari, Progress and problems in micro-grid protection schemes, Renewable and Sustainable Energy Reviews, 37, 834-839, 2014, DOI: 10.1016/j.rser.2014.05.044.
8. W.K.A. Najy, H.H. Zeineldin and W.L. Woon, Optimal protection coordination for microgrids with grid-connected and islanded capability, IEEE Transactions on Industrial Electronics, 60(4), 1668-1677, 2013, DOI: 10.1109/TIE.2012.2192893.
9. R.M. Kamel, A. Chaouachi and K. Nagasaki, Comparison the performances of three earthing systems for micro-grid protection during the grid connected mode, Smart Grid and Renewable Energy, 2(3), 206-215, 2011, DOI: 10.4236/sgre.2011.23024.
10. H.J. Laaksonen, Protection principles for future microgrids, IEEE Transactions on Power Electronics, 25(12), 2910–2918, 2010, DOI: 10.1109/TPEL.2010.2066990.
11. T.S. Ustun, C. Ozansoy and A. Zayegh, Modeling of a centralized microgrid protection system and distributed energy resources according to IEC 61850-70420, IEEE Transactions on Power Systems, 27(3), 1560–1567, 2012, DOI: 10.1109/TPWRS.2012.2185072.
12. S. Mirsaeidi, D. Mat Said, M. Wazir Mustafa, M. Hafiz Habibuddin and K. Ghaffari, An analytical literature review of the available techniques for the protection of micro-grids, International Journal of Electrical Power and Energy Systems, 58, 300-306, 2014, DOI: 10.1016/j.ijepes.2014.01.032.
13. D. Salomonsson, L. Soder and A. Saninno, Protection of low-voltage DC microgrids, IEEE Transactions on Power Delivery, 24(3), 1045-1053, 2009, DOI: 10.1109/TPWRD.2009.2016622.
14. B. Moeil, M. Gandomkar, M. Gooran and S. Mirsaeidi, Distinction of permanent and transient faults in microgrids using wavelet transform, Journal of Applied Environmental and Biological Sciences (JAEBS), 3(10), 41-51, 2013.
15. S.A. Gopalan, V. Sreeram and H.H.C. Lu, A review of coordination strategies and protection schemes for microgrids, Renewable and Sustainable Energy Reviews, 32, 222-228, 2014, DOI: 10.1016/j.rser.2014.01.037.
16. A. Oudalov and A. Fidigatti, Adaptive network protection in microgrids, International Journal of Distributed Energy Resources, 5, 201-225, 2009.
17. M. Dewadasa, Protection for distributed generation interfaced networks, Electrical Engineering, Faculty of Built Environment and Engineering, Queensland Univer-

sity of Technology, Queensland (Australia), 2010.
18. M. Dewadasa, R. Majumder, A. Ghosh and G. Ledwich, Control and protection of a microgrid with converter interfaced micro sources, in Power Systems, 2009. ICPS '09. International Conference on, Kharagpur, India, 2009.
19. R.M. Tumilty, M. Brucoli, and T.C. Green, Approaches to network protection for inverter dominated electrical distribution systems, in Proc. 3rd IET Int. Conf. Power Electron., Mach., Drives, 622–626, 2006.
20. M. A. Redfern and H. Al-Nasseri, Protection of microgrids dominated by distributed generation using solid state converters, in Proc. 9th Int. IET Conf. Developments Power Syst. Protection, 670–674, 2008.
21. N. Jayawarna, C. Jones, M. Barnes, and N. Jenkins, Operating microgrid energy storage control during network faults, in Proc. IEEE Int. Conf. Syst. Syst. Eng., 1–7, 2007.
22. N. Jayawarna, N. Jenkins, M. Barnes, M. Lorentzou, S. Papthanassiou, and N. Hatziargyriou, Safety analysis of a microgrid, in Proc. Int. Conf. Future Power Syst., 1–7, 2005.
23. E. Sortomme, S.S. Venkata and J. Mitra, Microgrid protection using communication-assisted digital relays, IEEE Transactions on Power Delivery, 25(4), 2789-2796, 2010, DOI: 10.1109/TPWRD.2009.2035810.
24. H. Nikkhajoei and R. Lasseter, Microgrid protection, in Proc. IEEE Power Eng. Soc. Gen. Meeting, 1–6, 2007.
25. M.A. Zamani, T.S. Sidhu and A. Yazdani, A protection strategy and microprocessor-based relay for low-voltage microgrids, IEEE Transactions on Power Delivery, 26(3), 1873-1883, 2011, DOI: 10.1109/TPWRD.2011.2120628.
26. E. Casagrande, W.L. Woon, H.H. Zeineldin and D. Svetinovic, A differential sequence component protection scheme for microgrids with inverter-based distributed generators, IEEE Transactions on Smart Grid, 5(1), 29-37, 2014, DOI: 10.1109/TSG.2013.2251017.
27. A.H. Etemadi and R. Iravani, Overcurrent and overload protection of directly voltage-controlled distributed resources in a microgrid, IEEE Transactions on Industrial Electronics, 60 (12), 5629-5638, 2013, DOI: 10.1109/TIE.2012.2229680.

ABOUT THE AUTHORS

Sohrab Mirsaeidi, Dalila Mat Said, Mohd. Wazir Mustafa, and **Mohd. Hafiz Habibuddin** are all with the Centre of Electrical Energy Systems (CEES), Faculty of Electrical Engineering (FKE), Universiti Teknologi Malaysia (UTM), 81310 Skudai, Johor, Malaysia.

Dalila Mat Said, also with the Centre of Electrical Energy Systems (CEES), Faculty of Electrical Engineering (FKE), Universiti Teknologi Malaysia (UTM), 81310 Skudai, Johor, Malaysia, is corresponding author, E-mail: dalilamatsaid@yahoo.com, Tel: 0060129732985.

Kimia Ghaffari is with Young Researchers and Elites Club, Saveh Branch, Islamic Azad University, Saveh, Iran.